

# The first total synthesis of (*R*)-convolutamydine A

Gianluigi Luppi,<sup>a</sup> Magda Monari,<sup>a</sup> Rodrigo J. Corrêa,<sup>b</sup> Flavio de A. Violante,<sup>b</sup> Angelo C. Pinto,<sup>b</sup> Bernard Kaptein,<sup>c</sup> Quirinus B. Broxterman,<sup>c</sup> Simon J. Garden<sup>b,\*</sup> and Claudia Tomasini<sup>a,\*</sup>

<sup>a</sup>Dipartimento di Chimica 'G. Ciamician'—Alma Mater Studiorum Università di Bologna, Via Selmi 2, 40126 Bologna, Italy

<sup>b</sup>Instituto de Química, Departamento de Química Orgânica, Universidade Federal do Rio de Janeiro, Ilha do Fundão, Bloco A, CT, Rio de Janeiro CEP 219450-900, Brazil

<sup>c</sup>DSM Research, Life Science—Advanced Synthesis and Catalysis, PO Box 18, 6160 MD Geleen, The Netherlands

Received 21 June 2006; revised 1 September 2006; accepted 21 September 2006

Available online 25 October 2006

**Abstract**—The first total synthesis of (*R*)-convolutamydine A has been achieved by the organocatalytic addition of acetone to 4,6-dibromoisatin. The absolute configuration was determined by single crystal X-ray diffraction. DFT studies were used to model the transition states for the aldol reaction and equilibrium geometries of the post-aldol reaction intermediates. The DFT study revealed that the aldol bond forming reaction was considerably endothermic.

© 2006 Elsevier Ltd. All rights reserved.

## 1. Introduction

Convolutamydines A–E are alkaloids that were isolated from the Floridian marine bryozoan *Amathia convoluta* in 1995.<sup>1</sup> These compounds have a 4,6-dibromo-3-hydroxyoxindole as a common skeleton and contain a quaternary stereocenter on C-3. Each convolutamydine differs in the side chain moiety at C-3, and for an enantioselective synthesis of these interesting natural products, the introduction of an asymmetric quaternary center is required. Several racemic syntheses of convolutamydines A–E have been proposed in the past,<sup>2</sup> and only very recently the enantioselective synthesis of convolutamydines B and E has been reported by Kobayashi and co-workers.<sup>3</sup> Here we report the first enantioselective synthesis of (*R*)-convolutamydine A (Fig. 1).

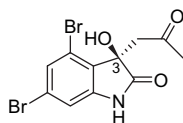


Figure 1. Structure of (*R*)-convolutamydine A.

**Keywords:** Convolutamydine A; Aldol reaction; Organocatalysis; DFT calculations.

\* Corresponding authors. Tel.: +39 0512099511; fax: +39 0512099456 (C.T.); tel.: +55 21 25627135; fax: +55 21 25627256 (S.J.G.); e-mail addresses: garden@iq.ufrj.br; claudia.tomasini@unibo.it

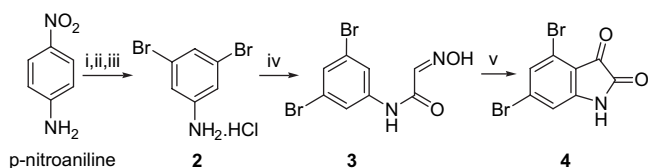
## 2. Results and discussion

Recently, we reported the first example of the enantioselective addition of acetone to isatin using organocatalysis.<sup>4</sup> Of the several prolinamides tested as catalysts, the best results were obtained using 10 mol % of *D*-Pro-(*R*)-β<sup>3</sup>-hPhg-OBn at –15 °C (up to 73% ee, (*R*)). In contrast, the results obtained with *L*-Pro-OH were quite unsatisfactory, affording the new stereogenic center with a maximum of 33% ee.

Interestingly, when *L*-Pro was used as catalyst, the *S* enantiomer was preferentially obtained. This outcome is opposite to that generally observed in the aldol addition of acetone to aldehydes when catalyzed by proline or prolinamides.<sup>5</sup> Moreover, the reaction catalyzed with our prolinamides afforded the new stereogenic center with greater ee and an absolute configuration that was dependent upon the absolute configuration of the proline moiety of the catalysts. In addition, the choice of the amino acid in the second position either enhances or reduces the enantiomeric excess and the yield.

Thus, we reasoned that, utilizing the same synthetic approach, we could readily obtain enantiomerically pure convolutamydine A. In this case, the starting material for the addition of acetone is 4,6-dibromoisatin, which is not commercially available, but can be obtained through a five-step sequence starting from *p*-nitroaniline, as previously reported for the total synthesis of racemic convolutamydine A<sup>2b</sup> (Scheme 1).

First, we investigated the *D*-Pro-OH catalyzed addition of acetone to **4** using various reaction conditions (Table 1).



**Scheme 1.** Reagents and yields: (i) AcOH, Br<sub>2</sub>, 98%; (ii) EtOH, NaNO<sub>2</sub>, H<sub>2</sub>SO<sub>4</sub>, 97%; (iii) EtOH, Raney Ni, H<sub>2</sub>, then HCl in H<sub>2</sub>O/EtOH, 86–96%; (iv) chloral, (H<sub>2</sub>NOH)<sub>2</sub>H<sub>2</sub>SO<sub>4</sub>, Na<sub>2</sub>SO<sub>4</sub>, H<sub>2</sub>O/EtOH (3:1, v/v), 82–88%; (v) 86% H<sub>2</sub>SO<sub>4</sub>, 80–86%.

**Table 1.** Enantiomeric excesses and yields of **1** obtained from the aldol reaction of 4,6-dibromoisatin with acetone catalyzed by D-proline<sup>a</sup>

Entry	Catalyst	Time (h)	Temp (°C)	Yield (%)	ee (%) <sup>b</sup>	Configuration
1	H-D-Pro-OH	17	20	Quant	3.5	<i>R</i>
2	H-D-Pro-OH	17	−15	86	55	<i>S</i>
3	H-D-Pro-OH <sup>c</sup>	16	−15	Quant	52	<i>S</i>
4	H-D-Pro-OH <sup>d</sup>	17	−15	45	35	<i>S</i>
5	H-D-Pro-OH	17	−30	0	—	—

<sup>a</sup> Conditions: the concentration of **4** in acetone was 0.15 M and 10 mol % of the catalyst was used.

<sup>b</sup> ee values were determined by HPLC.

<sup>c</sup> The concentration of **4** in acetone was 75 mM and 10 mol % of the catalyst was used.

<sup>d</sup> Dry acetone was used as the solvent.

As previously reported for isatin, the proline-catalyzed reaction afforded the desired product in good to excellent overall yield but with a moderate enantiomeric excess: at room temperature the reaction is very poorly enantioselective (entry 1), while the ee reaches 55% at −15 °C (entry 2). Furthermore, by lowering the temperature, the initial very poor (*R*)-enantioselectivity turns into a moderate (*S*)-enantioselectivity. This outcome is opposite to what we observed with the addition of acetone to isatin and is in agreement with the previously reported addition of acetone to aldehydes<sup>4,5</sup>. The proline catalyzed addition of acetone to 4-bromoisatin was therefore studied in detail by DFT calculations, as discussed later. As **4** is less soluble than isatin in acetone, the yield substantially improved when a lower concentration was used (entry 3 vs entry 2); on the other hand, when dry acetone was used, both a reduced yield and ee were obtained, thus suggesting that water may play a role in the reaction mechanism.

Owing to the unsatisfactory results, we tested the catalytic activity of a small library of dipeptides, which we considered to be the most interesting structures among those tested for the addition of acetone to isatins<sup>4</sup> (Fig. 2 and Table 2).

From Table 2 it can be seen that the optimal reaction temperature is −15 °C. The yields are always very high, with the exception of entry 7, where catalyst **9** was used, and of entry 16, where the catalyst loading was only 1 mol %. In general, catalysts containing the L-Pro-moiety preferentially afforded the (*S*)-enantiomer (entries 1, 2 and 7), while D-Pro-containing catalysts preferentially gave the (*R*)-enantiomer (entries 3, 4 and 8–17). An exception to this generalization was the reaction catalyzed by H-D-Pro-(*S*)-αMeChg-OBn **8**, which preferentially afforded the (*S*)-enantiomer (entries 5 and 6), but the ee is very low.

Finally, the total synthesis of (*R*)-convolutamydine A (**1**) was achieved using H-D-Pro-(*R*)-β<sup>3</sup>Phg-OBn **10** as the catalyst and by performing the reaction at a low concentration of **4** (entry 12). This favours the complete dissolution of **4** in the solvent (Scheme 2). Highly enantiomerically enriched (*R*)-

**Table 2.** Enantiomeric excesses and yields of convolutamydine A (**1**) obtained in the aldol reaction of **4** with acetone as catalyzed by dipeptides **5–11**<sup>a</sup>

Entry	Cat. <sup>b</sup>	Solvent	Time (h)	Temp (°C)	Yield (%)	ee (%) <sup>c</sup>	Configuration
1 <sup>d</sup>	<b>5</b>	Acetone	96	20	Quant	21	<i>S</i>
2 <sup>d</sup>	<b>6</b>	Acetone	96	20	Quant	28	<i>S</i>
3	<b>7</b>	Acetone	65	20	Quant	33	<i>R</i>
4 <sup>c</sup>	<b>7</b>	Acetone	16	−15	70	39	<i>R</i>
5	<b>8</b>	Acetone	65	20	Quant	4.5	<i>S</i>
6 <sup>e</sup>	<b>8</b>	Acetone	16	−15	82	9	<i>S</i>
7 <sup>d</sup>	<b>9</b>	Acetone	17	20	33	46	<i>S</i>
8	<b>10</b>	Acetone	17	20	Quant	54	<i>R</i>
9	<b>10</b>	Acetone	17	−15	Quant	62	<i>R</i>
10 <sup>d</sup>	<b>10</b>	Acetone	17	−15	90	60	<i>R</i>
11 <sup>d</sup>	<b>10</b>	Acetone	17	−30	91	50	<i>R</i>
12 <sup>c</sup>	<b>10</b>	Acetone	17	−15	Quant	68	<i>R</i>
13	<b>10</b>	Acetone/toluene	17	20	Quant	48	<i>R</i>
14	<b>10</b>	Acetone/toluene	17	−15	Quant	61	<i>R</i>
15 <sup>f</sup>	<b>10</b>	Acetone	17	−15	66	50	<i>R</i>
16 <sup>g</sup>	<b>10</b>	Acetone	17	−15	31	—	—
17 <sup>d</sup>	<b>11</b>	Acetone	96	20	Quant	34	<i>R</i>

<sup>a</sup> Unless otherwise specified, the concentration of **4** in acetone was 0.15 M.

<sup>b</sup> Unless otherwise stated, the catalyst loading was 10 mol %.

<sup>c</sup> ee values were determined by HPLC.

<sup>d</sup> Dry acetone was used as solvent.

<sup>e</sup> The concentration of **4** in acetone was 75 mM.

<sup>f</sup> The catalyst loading was 5 mol %.

<sup>g</sup> The catalyst loading was 1 mol %.

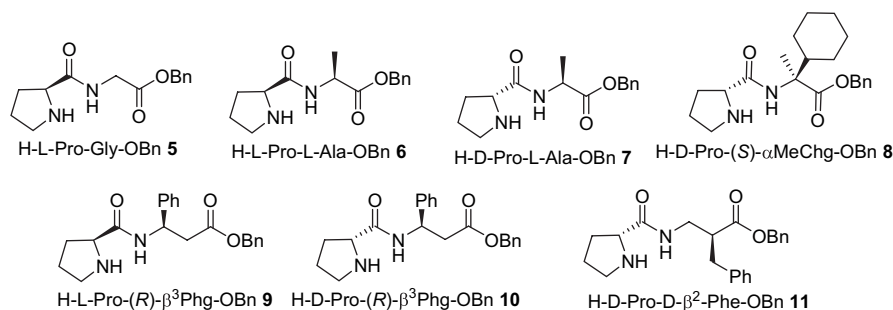
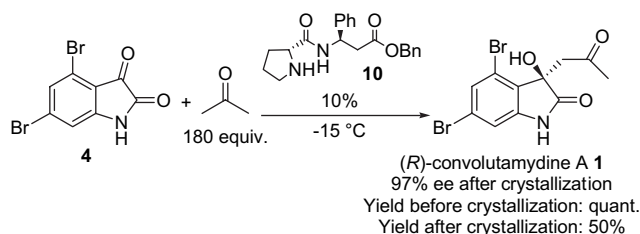


**Figure 2.** Dipeptides evaluated in this study.

(97% ee) was obtained after (a) elimination of the catalyst by filtration on silica; (b) partial crystallization resulting in the elimination of *rac*-**1** (due to the strong tendency of *rac*-**1** to self aggregate), thus reducing its solubility and enantiomerically enriching the solution in (*R*)-**1**; and (c) concentration of the mother liquors and crystallization. Several solvents were tested for the final crystallization, including methanol, diethyl ether, methyl *tert*-butyl ether, ethyl acetate, THF and toluene. Diethyl ether proved to be the most suitable solvent. The enantiomeric enrichment was analyzed by HPLC analysis (see Supplementary data). This process is quite simple and reproducible, and may therefore be applied for the production of larger quantities of **1**.



**Scheme 2.** Optimized synthesis of (*R*)-convolutamydine A.

Previously, the absolute configuration of natural convolutamydine A had only been assigned by CD correlation with similar compounds.<sup>6</sup> We have unambiguously determined the absolute configuration of our compound as (*R*) by single crystal X-ray diffraction (Fig. 3).

Comparison of the optical rotation of synthetic **1**,  $[\alpha]_{\text{D}}^{20} +41.4$  (*c* 0.14, MeOH), with the data for the optical rotation of the natural sample,  $[\alpha]_{\text{D}}^{20} +27.4$  (*c* 0.06, MeOH),<sup>1b</sup> confirms that the naturally occurring compound has the (*R*) configuration. However, we observed differences in the CD spectrum of **1** in methanol (Fig. 4) in comparison to the data reported in the literature.<sup>1b</sup> For the natural sample CD  $\lambda_{\text{ext}}$  (MeOH) at 228.20 nm was  $\Delta\epsilon -2.86$ , while we found  $\Delta\epsilon +25.86$  at the same wavelength. The complete CD spectrum of **1** is reported in Figure 4 and is very similar to the CD spectrum of convolutamydine B.<sup>3</sup>

The organocatalytic asymmetric proline-catalyzed aldol reaction has recently received considerable attention. In addition to the experimental results,<sup>5b,7</sup> DFT calculations have been found to be a persuasive argument for the nucleophilic addition of an enamine to the carbonyl group in preference to other reaction mechanisms and have been used to successfully predict and rationalize enantioselectivities.<sup>8</sup>

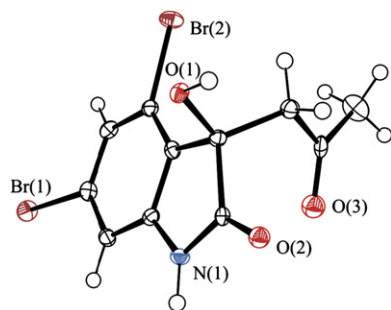


**Figure 3.** ORTEP drawing of the (*R*)-enantiomer of convolutamydine A.

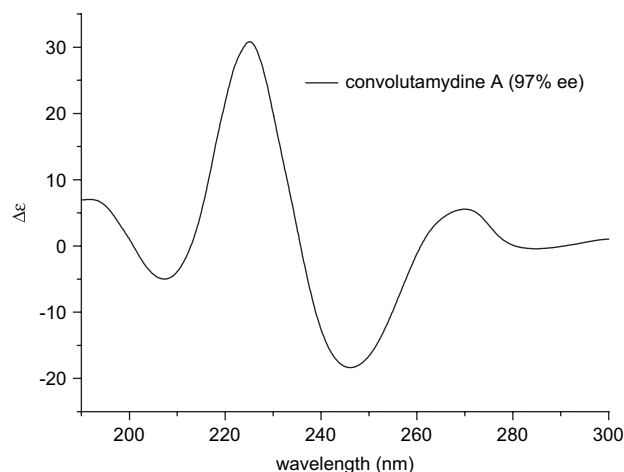


**Figure 4.** CD spectrum of a sample of **1** (concentration 5 mM in methanol).

Our experimental studies have revealed that the substrate 4,6-dibromoisatin gives an excellent yield with moderate enantiomeric excess for the (*S*)-enantiomer when using *D*-proline. In principle, this result could be explained using either a Houk–List transition state, involving an *anti*-enamine,<sup>5,9</sup> or via a *syn*-enamine.<sup>8i</sup> By simple examination of the structures, it was not immediately obvious how the presence of the adjacent amide group would affect the reaction outcome, although it was to be expected that the 4-bromo-substituent would impart a steric effect. Therefore, in order to obtain more insight into the proline-catalyzed addition of acetone to 4,6-dibromoisatin, combined semi-empirical (PM3)<sup>10</sup> followed by geometry/energy optimization using density functional theory (DFT, B3LYP)<sup>11</sup> 6-311G\*,<sup>12</sup> calculations were performed.

Previous DFT calculations have revealed the importance of a hydrogen bond between the carboxylic acid and the aldehyde or ketone carbonyl group. As the reaction progresses through the C···C bond forming transition state, this proton is simultaneously transferred to the forming alkoxide, ultimately giving rise to a zwitterionic, iminium, intermediate.

Initially, a PM3 conformer search of diastereoisomeric, zwitterionic, iminium intermediates was performed. A hydrogen bond between the carboxylate group and the tertiary alcohol was present as a result of the addition of the *anti*- or *syn*-hydrogen bonded *L*-proline enamines to the *Re* and *Si* faces of the keto-carbonyl group of isatin. The resulting unique lowest energy conformers were then modified by introduction of a 4-bromo-substituent, so as to model any steric effect of this substituent upon the aldol reaction, and subjected again to PM3 equilibrium geometry minimizations. These equilibrium geometry structures were then used as starting points for B3LYP/6-311G\* calculations, where the bromine atom was described by use of a pseudo-potential. From the initial eight inputs, seven unique equilibrium geometry structures (characterized as minima by the lack of any imaginary vibrations) were found (see Fig. 5 and Supplementary data).

In addition, the PM3 geometries of the 4-bromoisatin zwitterionic intermediates were used as starting points for determining PM3 transition state geometries for the retro-aldol

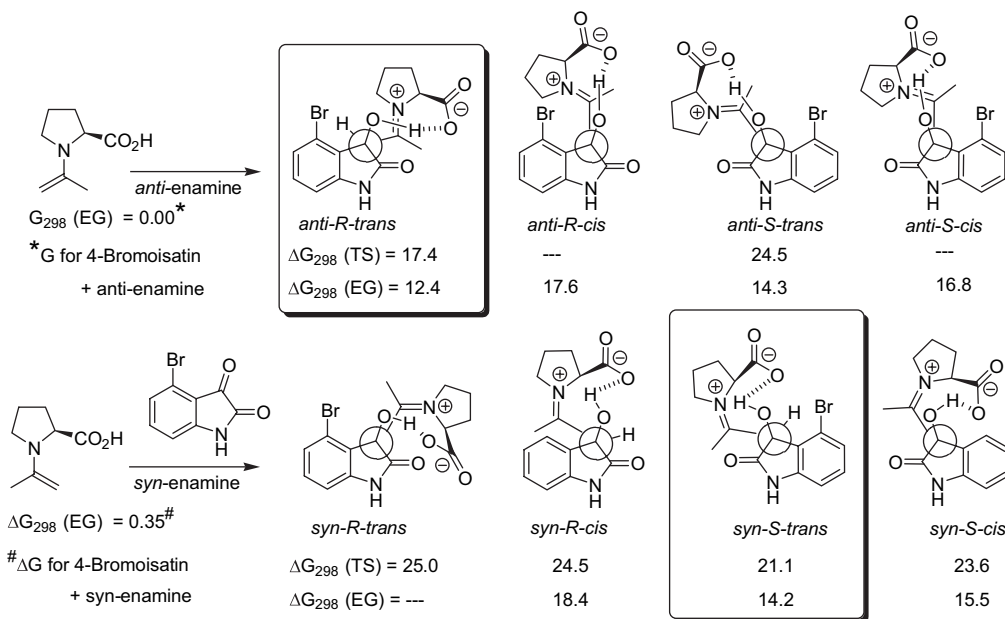


**Figure 5.** Schematic Newman projections of the eight lowest energy conformations resulting from the reaction of the *syn*-, and *anti*-, acetone L-proline enamines with 4-bromoisatin.<sup>13</sup>

reaction, which in turn were used as starting points for the B3LYP/6-311G\* transition state calculations. From the initial eight inputs, six unique transition states were found and were characterized by a single imaginary frequency that corresponded to simultaneous formation of the C–C bond and proton transfer from the acid to the forming alkoxide (see [Supplementary data](#)). The values of  $\Delta G$  for the respective transition states are presented in [Figure 5](#).

If the reaction of the acetone L-proline enamine with 4-bromoisatin was kinetically controlled, in accord with the calculated transition states, the *anti-R-trans* TS and *syn-S-trans* TS transition states would result in the (*R*)- and (*S*)-enantiomers, respectively, where the (*R*)-enantiomer would predominate.<sup>13</sup> This is consistent with the experimentally observed result. However, the calculated difference in free energy ( $\Delta G$ ) between these gas phase transition states would result in an enantiomeric excess considerably greater than that experimentally observed. This difference may in part be due to solvation effects reducing the energy difference between the transition states in solution.<sup>8i</sup> Interestingly, the calculations predict that the *syn*-enamine (*syn-S-trans* TS conformation) would be responsible for the formation of the minor enantiomer. Previous studies of proline-catalyzed intermolecular aldol reactions have generally attributed the formation of both major and minor products to the addition of the *anti*-enamine to the *Re* and *Si* faces of the aldehyde.<sup>8g</sup> Recently, Clemente and Houk, using DFT methods, have demonstrated for the Hajos–Parrish–Eder–Sauer–Wiechert reaction<sup>14</sup> that the respective *anti*-enamine leads to the major product and the respective *syn*-enamine to the minor product. In this case too,  $\Delta G$  was slightly overestimated by the theoretical model.<sup>8b,e</sup> Barbas et al. have also observed the importance of a *syn*-enamine (called *s-cis*, their work) in a diastereo- and enantioselective Mannich reaction.<sup>15</sup> In addition, our calculations show that the *syn-S-cis* TS structure is also lower in energy than the *anti-S-trans* TS.

Comparing our calculated transition structures, notable differences can be appreciated. The lowest energy transition state, *anti-R-trans* TS, has a staggered conformation of the substituents bonded to the carbons of the forming C···C bond. The *anti*-configuration of the enamine results in the proline moiety having a minimal steric interaction with both the bromine substituent of the aromatic ring and the amide group of the oxindole moiety. The O–C···C angle (112.3°) reflects considerable bond formation. This is consistent with the short bond length (1.661 Å) reflecting that the transition state resembles the product structure. In addition two electrostatic interactions can be identified:<sup>16</sup> (i) the forming alkoxide oxygen is stabilized by a proximal hydrogen of the pyrrolidine ring (2.258 Å) that is adjacent to the developing iminium ion ( $\delta^+\text{HCN}\cdots\text{O}^{\delta-}$ ); (ii) the amide carbonyl interacts with a methyl group hydrogen atom (2.503 Å),  $\delta^-\text{O}\cdots\text{CH}_3\text{C}=\text{N}^{\delta+}$ .

In the *syn-S-trans* TS the substituents bonded to the carbons involved in the forming C···C bond are staggered. This conformation further results in a minimal interaction with the bromine substituent. At the same time a possible steric interaction of the enamine methyl group with the amide carbonyl is minimized by the enamine being inclined away from the plane of the bromoisatin substrate (the angle of the forming C···C–O bond is 108.1° and the C···C distance is 1.975 Å), thus maximizing orbital overlap for the nucleophilic addition to the keto-carbonyl.<sup>17</sup> There are no notable secondary electrostatic interactions involved between the polar groups.

An unusual feature of this reaction is that the C···C bond forming step was found to be considerably endothermic, approximately 13 kcal/mol ([Fig. 6](#)). Therefore, the aldol reaction in this case could be reversible depending upon the energetics of the hydrolysis reaction. Clemente and Houk<sup>8e</sup> found that the hydrolysis transition state was 13 kcal/mol ( $\Delta H_0$ ) higher in energy than the initial reaction reagents

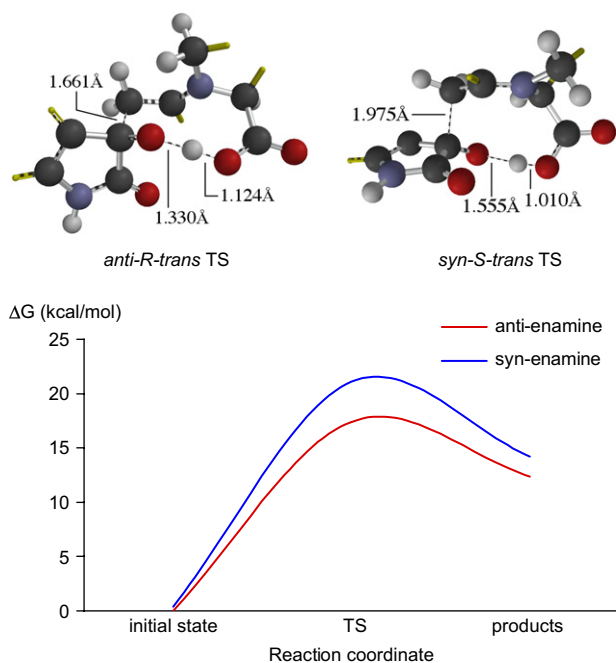


Figure 6. Reaction coordinate for the reaction of the *syn*- and *anti*-enamines.

but that this transition state was approximately 10 kcal/mol lower in energy than the aldol transition state.

Therefore, given the differences in the methodology between the studies, the activation energies ( $\Delta G_{298}$ ) for the aldol reaction are less than or similar to the previously cited aldol activation energy. Examining two extreme cases: (i) if the transition state for the hydrolysis reaction is lower in energy, then the transition state for the aldol reaction will not be reversible and the enantioselectivity of the reaction would be controlled by the aldol step. This is not in agreement with our experimental results. (ii) If the hydrolysis reaction passes through a transition state that is higher in energy than the aldol transition state, the C–C bond forming step can be reversible.

In this case, there are now two further situations that can result in control of the enantioselectivity: (i) the hydrolysis reaction and (ii) the intermediate zwitterionic iminium product ratio. Our calculations of the equilibrium geometry structures for the intermediate zwitterionic iminium products reveal a  $\Delta\Delta G$  of 1.45 kcal/mol favouring the *anti-R-trans*-EG.<sup>18</sup> This energy difference would correspond to an enantioselectivity of approximately 80%, which is much closer to the experimental result. Water has recently been observed to impart a beneficial effect upon the enantioselectivity of some amino acid catalyzed aldol reactions and is, evidently, involved in the hydrolysis step and at this point we cannot rule out the importance of the participation of water in the reaction mechanism.<sup>19</sup> Thus, the calculated reaction of the acetone L-proline enamine with 4-bromoisatin reveals several features: (i) the principal transition states have free energies of activation of 17 and 21 kcal/mol; (ii) the aldol bond forming reaction is endothermic; (iii) in the case of the transition state leading to the principle intermediate (*anti-R-trans* EG), the transition state has a resemblance to the product<sup>20</sup> greater than that found in previously studied reactions of the acetone proline enamine with aldehydes, as proved by a shorter C...C bond forming length.

In the case of the D-prolinamide dipeptides studied in this work, the (*R*)-aldol product was obtained, whereas with D-proline the (*S*)-aldol product was obtained. Due to the steric requirements of the catalyst **10**, we speculate that there must be a change in the reaction coordinate that inverts both the energy profile and the equilibrium geometries of the *syn-S-trans* (or *anti-S-trans*) and the *anti-R-trans* transition states.<sup>21</sup>

### 3. Conclusion

In conclusion, we have reported the first enantioselective synthesis of convolutamydine A (**1**), an alkaloid having interesting biological activity. The absolute configuration of the natural compound has been confirmed by an X-ray diffraction analysis of the synthetic sample. An initial theoretical investigation suggests that the major enantiomer can be explained as being formed via a Houk–List transition state involving the *anti*-enamine but the minor enantiomer is the result of reaction of the *syn*-enamine. In addition, the enantioselectivity of the reaction does not appear to be controlled by the aldol transition states.

## 4. Experimental

### 4.1. General

Routine NMR spectra were recorded with spectrometers at 400, 300 or 200 MHz (<sup>1</sup>H NMR) and at 100, 75 or 50 MHz (<sup>13</sup>C NMR). Chemical shifts are reported in  $\delta$  values relative to the solvent peak of CHCl<sub>3</sub>, set at 7.27 ppm. Infrared spectra were recorded with an FTIR spectrometer. Melting points were determined in open capillaries and are uncorrected. The CD spectra were obtained using cylindrical fused quartz cells of 0.1 cm path length. The values are expressed in terms of molecular CD.

D-Proline is commercially available. L- $\alpha$ -Methylcyclohexylglycine has been prepared by hydrogenation of L-( $\alpha$ -methyl)-phenylglycine as described previously.<sup>22</sup> The  $\beta$ -amino acids R- $\beta^3$ -hPhg (L- $\beta^3$ -homophenylglycine) and L- $\beta^2$ -hPhe (L- $\beta^2$ -homophenylalanine) were prepared at DSM Research as described in PCT Pat. Appl. WO 01/42173 and Eur. Pat. Appl. No. 04075597.7 (patent pending), respectively. Peptide bond formation was accomplished via standard solution-phase procedures, with HBTU [*O*-(benzotriazol-1-yl)-*N,N,N',N'*-tetramethyluronium hexafluorophosphate] and triethylamine in acetonitrile on Boc-protected prolines. The removal of the Boc group was accomplished via reaction with trifluoroacetic acid in dichloromethane.

Analytical high performance liquid chromatograph (HPLC) was performed on an HP 1090 liquid chromatograph equipped with a variable wavelength UV detector (deuterium lamp 190–600 nm), using an AD column (0.46 cm I.D.  $\times$  25 cm) (Daicel Inc.) for the analysis of ee values of convolutamydine A. Elution conditions: flow rate 0.7 mL/min, solvent hexane/isopropanol 80:20, retention time: 16.7 min for isomer *S* and 21.5 min for isomer *R*, detection wavelength 225 and 230 nm. Hexane CHROMASOLV<sup>®</sup> and isopropanol CHROMASOLV<sup>®</sup> for HPLC were used as the eluting solvents.

## 4.2. Optimized synthesis of (*R*)-convolutamydine A

H-D-Pro-*R*- $\beta^3$ -hPhg-OBn (0.03 mmol, 11 mg) was stirred in acetone (4 mL) for 15 min at  $-15^\circ\text{C}$ . Solid 4,6-dibromoisatin<sup>2b</sup> (0.3 mmol, 91 mg) was added and the mixture was stirred for 17 h. After this time, acetone was removed under reduced pressure and the mixture was purified by flash chromatography (cyclohexane/ethyl acetate 1:1), to eliminate the catalyst and enhance the enantiomeric excess.<sup>23</sup> The enantiomeric excesses were determined by HPLC prior to purification. Pure (*R*)-convolutamydine A was obtained from the enriched enantiomeric mixture, by crystallization from diethyl ether. Yield before crystallization: quantitative. Yield after crystallization: 50%; mp=196–201  $^\circ\text{C}$ , lit.<sup>2</sup> 190–195  $^\circ\text{C}$ ;  $[\alpha]_D^{20}$  +41.4 (*c* 0.14, MeOH) lit.<sup>2</sup>:  $[\alpha]_D^{20}$  +27.4 (*c* 0.06, MeOH); IR (CHCl<sub>3</sub>, 3.10<sup>-3</sup> M):  $\nu$ =3428, 3244, 1740, 1720, 1614 cm<sup>-1</sup>; <sup>1</sup>H NMR (300 MHz, CDCl<sub>3</sub>):  $\delta$  2.18 (s, 3H), 3.35 (d, 1H, *J*=17.1 Hz), 3.74 (d, 1H, *J*=17.1 Hz), 7.01 (s, 1H), 7.33 (s, 1H), 7.84 (br s, 1H); <sup>1</sup>H NMR (300 MHz, CD<sub>3</sub>OD):  $\delta$  2.13 (s, 3H), 3.31 (d, 1H, *J*=17.7 Hz), 4.01 (d, 1H, *J*=17.7 Hz), 7.06 (d, 1H, *J*=1.8 Hz), 7.33 (d, 1H, *J*=1.8 Hz); <sup>13</sup>C NMR (75 MHz, CD<sub>3</sub>OD):  $\delta$  28.9, 74.5, 112.6, 119.3, 123.3, 128.0, 128.4, 146.3, 178.9, 206.0; <sup>13</sup>C NMR (75 MHz, CDCl<sub>3</sub>):  $\delta$  30.0, 47.7, 75.2, 113.3, 129.5, 144.2, 162.5, 177.2, 182.6; MS (EI) *m/z* (rel intensity) 365, 363, 361, 320, 308, 306, 304, 277, 275, 254, 168; HRMS (EI) calcd for C<sub>11</sub>H<sub>9</sub><sup>79</sup>Br<sub>2</sub>NO<sub>3</sub> (M<sup>+</sup>): 360.8949; found: 360.8941.

The enantiomeric excess could be further improved by the crystallization of *rac*-1 from Et<sub>2</sub>O, leaving an ethereal solution of (*R*)-1. Concentration of this solution gave a crystalline product of 97% ee as determined by HPLC and crystals suitable for X-ray diffraction were obtained.

## 4.3. X-ray crystallography

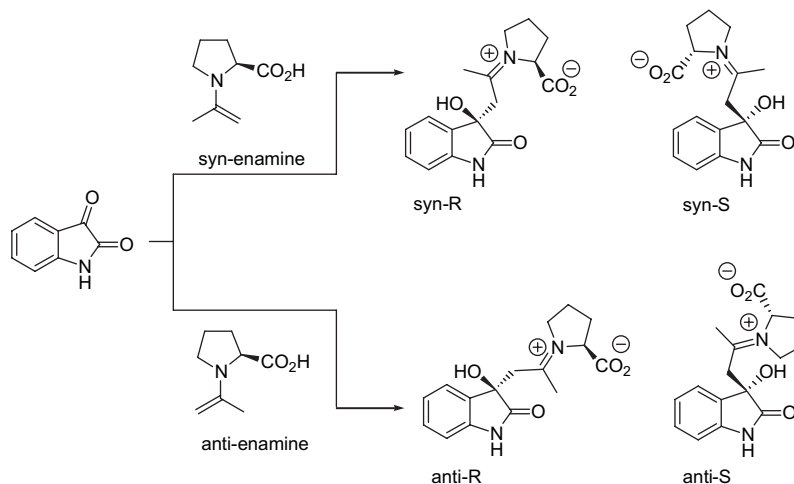
The X-ray intensity data for convolutamydine A<sup>24</sup> were measured on an AXS ApexII diffractometer, equipped with a CCD detector. Cell dimensions and the orientation matrix were initially determined from a least-squares refinement on reflections measured in three sets of 20 exposures, collected in three different  $\omega$  regions, and eventually refined against all data. For both crystals, a full sphere of reciprocal

space was scanned by 0.3 $^\circ$   $\omega$  steps. The software SMART was used for collecting frames of data, indexing reflections and determination of lattice parameters. The collected frames were then processed for integration by the SAINT program, and an empirical absorption correction was applied using SADABS. The structure was solved by direct methods and subsequent Fourier syntheses in the orthorhombic crystal system (space group *P*212121) and refined by full-matrix least-squares on F<sup>2</sup> (SHELXTL), using anisotropic thermal parameters for all non-hydrogen atoms. All hydrogens, except those attached to the nitrogen and oxygen atoms, which were located in the Fourier map, were added in calculated positions, included in the final stage of refinement with isotropic thermal parameters,  $U(\text{H})=1.2U_{\text{eq}}(\text{C})$  [ $U(\text{H})=1.5U_{\text{eq}}(\text{C}-\text{Me})$ ], and allowed to ride on their carrier carbons. The absolute configuration was determined (Flack parameter  $-0.006(8)$ ).

## 4.4. Methodology for obtention of the initial inputs for the DFT calculations—semi-empirical PM3 calculations

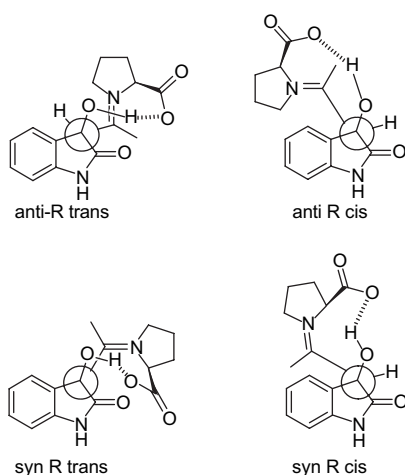
Initially, a PM3 conformer search on two of the four possible diastereoisomeric zwitterionic iminium intermediates (*syn*-*S*, attack of the *syn*-enamine on the *Re*-face of the ketone, and *anti*-*R*, attack of the *anti*-enamine on the *Si* face of the ketone) was performed (Scheme 3).

In each case, two structurally different, lowest energy, conformers were found. In short, these isomers can be described as having the proline moiety *cis* or *trans* to the aromatic ring of the oxindole nucleus. These isomers are related by rotation around the C–C bond formed in the aldol reaction and the carboxylate group forms a hydrogen bond to the alcohol that is either proximal (*cis*) or distal (*trans*) to the aromatic ring. These isomeric structures could, in principle, be traced back to initial reactant Van der Waals complexes where a hydrogen bond from the carboxylic acid could occur to either side of the keto-carbonyl group. The four isomers were then used to model the *syn*-*R* and *anti*-*S* structures by inverting the stereochemistry of the tertiary alcohol and performing equilibrium geometry PM3 calculations (Scheme 4). Thus, a total of eight equilibrium geometry zwitterionic intermediates were obtained. 4,6-Dibromoisatin was modeled as the 4-bromoisatin to ensure that any steric effect



**Scheme 3.** Reaction of the *syn*-, and *anti*-, acetone L-proline enamines with isatin resulting in four diastereomeric zwitterionic intermediates.

due to the bromine was incorporated. The eight equilibrium geometry PM3 structures obtained for isatin were modified by substitution of 4-H for 4-Br and subjected to PM3 equilibrium geometry calculations. These equilibrium geometry structures were then used as starting points for B3LYP 6-311G\* calculations, where the bromine atom was described by use of a pseudopotential. From the initial eight inputs, seven unique equilibrium geometry structures (characterized as minima by the lack of any imaginary vibrations) were found.



**Scheme 4.** Schematic Newman projections of the four conformations for the zwitterionic intermediates *anti-R* and *syn-R* that would lead to formation of the *R*-enantiomer of the aldol product. Hydrogens behind the plane of the oxindole nucleus bonded to the carbon of the enamine have been omitted for clarity. The descriptors ‘trans’ and ‘cis’ are used, subjectively, to indicate the position of the proline nucleus relative to the aromatic ring of the oxindole nucleus.

In addition, the PM3 geometries of the 4-bromoisatin zwitterionic intermediates were used as starting points for determining PM3 transition state geometries for the retro-aldol reaction. The eight PM3 aldol transition states were used as starting points for the B3LYP 6-311G\* transition state calculations. From the initial eight inputs, six unique transition states were found that were characterized by a single imaginary frequency that corresponded to simultaneous formation of the C–C bond and proton transfer from the acid to the forming alkoxide.

### Acknowledgements

G.L. and C.T. thank MIUR (PRIN 2004), CNR-ISOF and University of Bologna (Funds for selected topics) for financial support. S.J.G., R.J.C., A.C.P. and F.A.V. wish to thank CAPES, CNPq and FAPERJ for financial support. S.J.G. gratefully acknowledges Dr. Pierre Esteves, Instituto de Química, Universidade Federal do Rio de Janeiro, for helpful discussion.

### Supplementary data

Experimental details and characterization data of the catalysts **5–11**. Cartesian coordinates, structures, and tables

of thermodynamic data from the DFT calculations. Supplementary data associated with this article can be found in the online version, at [doi:10.1016/j.tet.2006.09.077](https://doi.org/10.1016/j.tet.2006.09.077).

### References and notes

- (a) Zhang, H.-P.; Shigemori, H.; Ishibashi, M.; Kosaka, T.; Pettit, G. R.; Kamano, Y.; Kobayashi, J. *Tetrahedron* **1994**, *50*, 10201–10206; (b) Kamano, Y.; Zhang, H.-P.; Ichihara, Y.; Kizu, H.; Komiyama, K.; Pettit, G. R. *Tetrahedron Lett.* **1995**, *36*, 2783–2784; (c) Zhang, H.-P.; Kamano, Y.; Ichihara, Y.; Kizu, H.; Komiyama, K.; Itokawa, H.; Pettit, G. R. *Tetrahedron* **1995**, *51*, 5523–5528.
- (a) Kawasaki, T.; Nagaoka, M.; Satoh, T.; Okamoto, A.; Ukon, R.; Ogawa, A. *Tetrahedron* **2004**, *60*, 3493–3503; (b) Garden, S. J.; Torres, J. C.; Ferreira, A.; Silva, R. B.; Pinto, A. C. *Tetrahedron Lett.* **1997**, *38*, 1501–1504; (c) Jnaneshwar, G. K.; Bedekar, A. V.; Deshpande, V. H. *Synth. Commun.* **1999**, *29*, 3627–3633; (d) Jnaneshwar, G. K.; Deshpande, V. H. *J. Chem. Res., Synop.* **1999**, 632–633.
- Nakamura, T.; Shirokawa, S.-I.; Hosokawa, S.; Nakazaki, A.; Kobayashi, S. *Org. Lett.* **2006**, *8*, 677–679.
- Luppi, G.; Cozzi, P. G.; Monari, M.; Kaptein, B.; Broxterman, Q. B.; Tomasini, C. *J. Org. Chem.* **2005**, *70*, 7418–7421.
- (a) List, B.; Lerner, R. A.; Barbas, C. F. *J. Am. Chem. Soc.* **2000**, *122*, 2395–2396; (b) Sakthivel, K.; Notz, W.; Bui, T.; Barbas, C. F. *J. Am. Chem. Soc.* **2001**, *123*, 5260–5267.
- Takayama, H.; Shimizu, T.; Sada, H.; Harada, Y.; Kitajima, M.; Aimi, N. *Tetrahedron* **1999**, *55*, 6841–6846.
- (a) List, B.; Hoang, L.; Martin, H. J. *Proc. Natl. Acad. Sci. U.S.A.* **2004**, *101*, 5839–5842; (b) Hoang, L.; Bahmanyar, S.; Houk, K. N.; List, B. *J. Am. Chem. Soc.* **2003**, *125*, 16–17; (c) List, B. *Synlett* **2001**, 1675–1686.
- (a) Bahmanyar, S.; Houk, K. N.; Martin, H. J.; List, B. *J. Am. Chem. Soc.* **2003**, *125*, 2475–2479; (b) Clemente, F. R.; Houk, K. N. *J. Am. Chem. Soc.* **2005**, *127*, 11294–11302; (c) Bassan, A.; Zou, W. B.; Reyes, E.; Himo, F.; Cordova, A. *Angew. Chem., Int. Ed.* **2005**, *44*, 7028–7032; (d) Arno, M.; Zaragoza, R. J.; Domingo, L. R. *Tetrahedron: Asymmetry* **2005**, *16*, 2764–2770; (e) Clemente, F. R.; Houk, K. N. *Angew. Chem., Int. Ed.* **2004**, *43*, 5766–5768; (f) Cheong, P. H. Y.; Houk, K. N.; Warriar, J. S.; Hanessian, S. *Adv. Synth. Catal.* **2004**, *346*, 1111–1115; (g) Allemann, C.; Gordillo, R.; Clemente, F. R.; Cheong, P. H. Y.; Houk, K. N. *Acc. Chem. Res.* **2004**, *37*, 558–569; (h) Bahmanyar, S.; Houk, K. N. *Org. Lett.* **2003**, *5*, 1249–1251; (i) Rankin, K. N.; Gauld, J. W.; Boyd, R. J. *J. Phys. Chem. A* **2002**, *106*, 5155–5159; (j) Arno, M.; Domingo, L. R. *Theor. Chem. Acc.* **2002**, *108*, 232–239; (k) Bahmanyar, S.; Houk, K. N. *J. Am. Chem. Soc.* **2001**, *123*, 12911–12912.
- (a) Jung, M. E. *Tetrahedron* **1976**, *32*, 3–31; (b) Notz, W.; List, B. *J. Am. Chem. Soc.* **2000**, *122*, 7386–7387; (c) Cordova, A.; Notz, W.; Barbas, C. F. *J. Org. Chem.* **2002**, *67*, 301–303.
- All PM3 calculations were performed using Spartan’02 Wavefunction, Inc., Irvine, CA.
- (a) Becke, A. D. *J. Chem. Phys.* **1993**, *98*, 1372–1377; (b) Lee, C.; Yang, W.; Parr, R. G. *Phys. Rev. B* **1988**, *37*, 785–789.
- Frisch, M. J., et al. *Gaussian 98, Revision A.9*; Gaussian, Inc.: Pittsburgh, PA, 1998; Calculations were performed at B3LYP/6-311G\* for C, H, N and O and Lanl2dz for the Br atom. The complete citation is given in [Supplementary data](#).

13. The corresponding values of  $\Delta G$  for the diastereomeric aldol transition states (TS) and for the respective intermediate zwitterionic iminium ion product equilibrium geometries (EG) are given relative to  $\Sigma G$  for the substrates 4-bromoisatin+anti-enamine. The hydrogens behind the plane of the oxindole moiety bonded to the carbon of the enamine and the 4-bromoatom of the products *syn-R-cis* and *syn-S-cis* have been omitted for clarity. The descriptors trans and cis are used, subjectively, to indicate the position of the proline nucleus relative to the aromatic ring of the oxindole nucleus.
14. (a) Hajos, Z. G.; Parrish, D. R. *J. Org. Chem.* **1974**, *39*, 1615–1621; (b) Hajos, Z.G.; Parrish, D.R. German Patent DE 2102623, 1971; (c) Eder, U.; Sauer, G.; Wiechert, R. German Patent DE 2014757, 1971; (d) Eder, U.; Sauer, G.; Wiechert, R. *Angew. Chem., Int. Ed. Engl.* **1971**, *10*, 496–497; (e) Ruppert, J.; Eder, U.; Wiechert, R. *Chem. Ber.* **1973**, *106*, 3636–3644.
15. Cheong, P. H. Y.; Zhang, H. L.; Thayumanavan, R.; Tanaka, F.; Houk, K. N.; Barbas, C. F. *Org. Lett.* **2006**, *8*, 811–814.
16. Cannizzaro, C. E.; Houk, K. N. *J. Am. Chem. Soc.* **2002**, *124*, 7163–7169.
17. (a) Burgi, H. B.; Dunitz, J. D.; Shefter, E. *J. Am. Chem. Soc.* **1973**, *95*, 5065–5067; (b) Burgi, H. B.; Dunitz, J. D.; Lehn, J. M.; Wipff, G. *Tetrahedron* **1974**, *30*, 1561–1572; (c) Burgi, H. B.; Dunitz, J. D. *Acc. Chem. Res.* **1983**, *16*, 153–161.
18. Where there is thermodynamic control then the product ratio is given by the respective equilibrium constants.  $\Delta\Delta G/RT = -\ln(K_1/K_2)$ .
19. (a) Cordova, A.; Zou, W. B.; Ibrahim, I.; Reyes, E.; Engqvist, M.; Liao, W. W. *Chem. Commun.* **2005**, 3586–3588; (b) Mase, N.; Nakai, Y.; Ohara, N.; Yoda, H.; Takabe, K.; Tanaka, F.; Barbas, C. F. *J. Am. Chem. Soc.* **2006**, *128*, 734–735; (c) Pihko, P. M.; Laurikainen, K. M.; Usano, A.; Nyberg, A. I.; Kaavi, J. A. *Tetrahedron* **2006**, *62*, 317–328.
20. Hammond, G. S. *J. Am. Chem. Soc.* **1955**, *77*, 334–338.
21. Initial PM3 conformer analyses suggest that the acetone derived enamine from catalyst **10** may have a cavity in which a substrate may dock, thus giving these catalysts a truly biomimetic nature.
22. (a) Formaggio, F.; Moretto, V.; Crisma, M.; Toniolo, C.; Kaptein, B.; Broxterman, Q. B. *J. Peptide Res.* **2004**, *63*, 161–170; (b) Kruizinga, W. H.; Bolster, J.; Kellogg, R. M.; Kamphuis, J.; Boesten, W. H. J.; Meijer, E. M.; Schoemaker, H. E. *J. Org. Chem.* **1988**, *53*, 1826–1827; (c) Kaptein, B.; Boesten, W. H. J.; Broxterman, Q. B.; Peters, P. J. H.; Schoemaker, H. E.; Kamphuis, J. *Tetrahedron: Asymmetry* **1993**, *4*, 1113–1116.
23. (a) Stefani, R.; Cesare, V. *J. Chromatogr., A* **1998**, *813*, 79–84; (b) Lozà, E.; Lojà, D.; lemme, A.; Freimanis, J. *J. Chromatogr., A* **1995**, *708*, 231–243.
24. Crystal data for convolutamydine A. The crystals were obtained from diethyl ether. Formula weight: 363.01; orthorhombic,  $P2_12_12_1$ ;  $Z=4$ ;  $a=7.61 \text{ \AA}$ ;  $b=7.91 \text{ \AA}$ ;  $c=19.83 \text{ \AA}$ ;  $\alpha=\beta=\gamma=90^\circ$ ;  $V=1193.14 \text{ \AA}^3$ ; 2884 unique reflections;  $R=0.0168$ . The structure has been deposited with the Cambridge Crystallographic Data Centre and has received the deposition number CCDC 610173.